Solar Energy 184 (2019) 148–152

Contents lists available at ScienceDirect

Solar Energy

journal homepage: www.elsevier.com/locate/solener

Transformations in the Mn-O-Si system using concentrated solar energy

D. Fernández-González[a,*], J. Prazuch[b], I. Ruiz-Bustinza[c], C. González-Gasca[d], J. Piñuela-Noval[a], L.F. Verdeja[a]

[a] Department of Materials Science and Metallurgical Engineering, School of Mines, Energy and Materials, University of Oviedo, Oviedo, Asturias, Spain
[b] Department of Physical Chemistry and Modelling, Faculty of Materials Science and Ceramics, AGH University of Science and Technology, Krakow, Poland
[c] Department of Geological and Mining Engineering, Polytechnic University of Madrid, Madrid, Spain
[d] European University of Madrid-Laureate International Universities, Villaviciosa de Odón, Madrid, Spain

ARTICLE INFO

Keywords:
Concentrated solar energy
Manganese
Ferroalloys
Environment
Silicomanganese

ABSTRACT

Energy consumption and carbon dioxide emissions are a problem in the metallurgical industries. The synthesis of manganese and silicomanganese using concentrated solar energy is proposed in this paper. Mixtures of oxide of manganese (IV) and silicon (50 wt% and 75 wt%) were treated in a 1.5 kW solar furnace located in Odeillo. Results demonstrated that mixtures of manganese and silicon, but also silicomanganese, are obtained after treatment even in the less favorable situation: without iron, which reduces the liquidus temperature, and without slag-forming reagents.

1. Introduction

The utilization of the solar energy in the field of materials has been studied for many years (Fernández-González et al., 2018a). The main reason that explains this interest is that high temperatures can be reached without paying for either fossil fuels or electricity and, in this way, processes might be less expensive and environmentally friendly. Our research group has used concentrated solar energy in different applications in the field of materials: in the synthesis of calcium aluminates (Fernández-González et al., 2018b), in the indirect reduction of mill scale to produce high quality magnetite (Ruiz-Bustinza et al., 2013), in the direct reduction of iron oxides (laboratory quality reagents, Mochón et al. (2014), Fernández-González et al. (2018c); real iron ore sinter, Fernández-González et al. (2018c)); in the treatment of Basic Oxygen Furnace slag (Fernández-González et al. (2019a); and in the synthesis of silicon calcium alloy (Fernández-González et al. (2019b).

85–90% of the manganese is consumed in the steel industry (Zhang and Cheng, 2007). The production of steel was doubled in the last twenty years (800 Mt in 1999 to 1689 Mt in 2017), and thus the production of manganese has grown at the same rate (7.5 Mt in 1999 16 Mt in 2017) (United States Geological Survey; Holappa 2013). The growing demand of manganese has led the manganese metallurgical industries to the utilization of both low grade manganese ores and secondary manganese resources (Zhang and Cheng, 2007; Olsen et al., 2007; Tangstad, 2013). In this way, Fernández-González et al. (2018d) studied the recovery of manganese from anodic lodes and scrapings generated in the zinc electrolysis process. As a result of the process of Fernández-González et al. (2018d) electrolytic manganese, manganese oxide (II) and manganese oxide (IV) could be obtained. However, the production of electrolytic manganese, the same as the production of silicomanganese, is energy intensive (Sakamoto et al., 1999; Holappa, 2013; Haque and Norgate, 2013), and searching for alternative processes using less expensive and more environmentally friendly energy sources is the aim of the researchers in the field of the ferroalloys. One of the possibilities is the silicothermic reduction.

The silicothermic reduction of iron ore and slag rich in MnO is used in the commercial production of medium carbon ferromanganese (Ndlovu et al., 2017; Olsen et al., 2007). The kinetics for the silicothermic reduction of the manganese oxide in MnO-SiO_2-CaO-Al_2O_3 slags was studied by Jamieson and Coley (2017) in the range of temperatures 1550–1650 °C. Similarly, Heo and Park (2018) studied the recovery of manganese by silicothermic reduction of BaO-MnO-MgO-CaF_2 slags at high temperatures. These researchers proposed the silicothermic reduction of manganese oxides from slags at high temperatures using conventional furnaces. The silicothermic reduction could be performed using solar furnaces to recover manganese from slags rich in manganese. This way, the high temperatures required for the process would be reached without paying for electricity or fossil fuels.

In this manuscript we propose the obtaining of manganese and/or silicomanganese using both the concentrated solar energy and the silicothermic reduction of manganese oxide (IV). This way, energy costs

* Corresponding author.
E-mail address: fernandezgdaniel@uniovi.es (D. Fernández-González).

https://doi.org/10.1016/j.solener.2019.04.004
Received 18 January 2019; Received in revised form 27 March 2019; Accepted 1 April 2019

Fig. 1. (a) Solar furnace used in the experiments; (b) presence of liquid phase in the crucibles during the experiments.

might be reduced in the ferroalloys industry. Future researches might be also focused on the recovery of manganese from ferromanganese and silicomanganese slags to strive towards a circular economy in the ferroalloys industry.

2. Materials and methods

The experiments were performed in the vertical axis solar furnace of 1.5 kW (maximum power) located in Odeillo (France) and belonging to the PROMES-CNRS (Procédés, Matériaux et Énergie Solaire-Centre National de la Recherche Scientifique) (Fig. 1a). The heliostat directed the incident radiation towards the parabolic concentrator which made the radiation converge in a focal surface of 15 mm in diameter. Thus, the incident radiation was concentrated a maximum of 15,000 times. The incident radiation varied within 776 and 937 W/m^2 in all experiments. Two sets of experiments were performed in the solar furnace: one of three tests with 50 wt% Si (Mn7, Mn8 and Bonus50) and the other of three with 75 wt% Si (Mn9, Mn10 and Bonus75). The values of incident radiation in each sample were (in W/m^2): Mn7, 937; Mn8, 840; Bonus50, 910; Mn9, 898; Mn10, 812; Bonus75, 776. The power (P) can be calculated using the following equation:

$$P(W) = IR\,(W/m^2)\cdot 1.5\cdot ShOp/100$$

where IR is the incident radiation and ShOp is the shutter opening value. The power was progressively applied using the shutter opening to minimize the violent reactions. In the case of the samples with 50 wt % Si, the value of the ShOp was: 25 (0–1 min), 40 (1–3 min), 51 (3–5 min), 60 (5–8 min) and 74 (8–12 min). In the case of the samples with 75 wt% Si, the value of the ShOp was: 25 (0–1 min), 40 (1–3 min), 51 (3–5 min), 60 (5–8 min), 74 (8–12 min), and 90 (12–15 min). After this heating program the sample was air cooled down to the room temperature.

Samples were prepared using laboratory quality reagents, oxide of manganese (IV) and metallurgical silicon (99.9%), in the following proportions 50 wt% Si and 75 wt% Si to define the two types of samples. Mixtures were loaded into tabular alumina crucibles of 55 mm in height, 30 mm upper diameter, 25 mm lower diameter and 3 mm of wall thickness. The crucible with the sample was located inside a glass chamber connected to a pump that ensured a pressure of 0.85 atm inside of the chamber, but the atmosphere inside was the ambient one (oxidizing). The objective of using the glass chamber was to avoid the damage of the parabolic concentrator. Temperature was indirectly measured using a thermocouple of cromel-alumel located at an average height outside of the crucible. Using finite element based software we calculated that the temperature in the layer in contact with the solar beam and in a depth of 5–10 mm was > 1700 °C. Moreover, we observed molten phase in the crucibles during the experiments (Fig. 1b), but in a depth of 12–15 mm from the surface of the load the material remained unreacted (powdered).

3. Results and discussion

3.1. Results

Agglomerated pieces of 12–15 mm were removed from the crucible after the treatment. These pieces were cut into four small pieces: two of them were used for X-ray diffraction analysis (pieces were powdered); the other two were used for Scanning Electron Microscopy – Energy Dispersive X-ray spectroscopy. X-ray diffraction measurements of powdered samples were conducted with Empyrean PANalytical diffractometer using Kα1 and Kα2 radiation from Cu anode. All measurements were performed with Bragg-Brentano setup at room temperature with the 0.006° step size at 5–90° 2θ scanning range and the 145 s of measurement time for each step. Data analysis and the peak profile fitting procedure were carried out using XPowder12 Ver. 01.02 (Database PDF2 (70–0.94)). X-ray diffraction patterns are presented in Fig. 2 (Mn7), Fig. 3 (Mn8), Fig. 4 (Bonus50), Fig. 5 (Mn9), Fig. 6 (Mn10) y Fig. 7 (Bonus75).

X-ray diffraction analyses show that manganese was obtained in all samples, which together with the silicon added in excess, forms the mixtures silicon-manganese. Additionally, silica, product of the silicothermic reduction of the manganese oxide (IV), is also detected in all samples. Furthermore, silica can be also produced as a result of the silicon oxidation in the oxidizing atmosphere used in the experiments. As minority phases we can indicate different silicomanganese compounds (Mn_5Si_3, Mn_7Si, $Mn_{15}Si_{26}$ and $Mn_{27}Si_{47}$), partially reduced manganese oxides (MnO, Mn_2O_3, Mn_3O_4 and Mn_5O_8) and manganese silicate (Mn_2SiO_4).

Results were also checked using the scanning electron microscope with possibility of performing point analysis (SEM-EDX). A micrograph of the sample Mn7 is shown in the Fig. 8, while the results of the point analysis (Fig. 8) are presented in the Table 1. Points 1 and 2 would represent the mixtures silicon-manganese detected in the X-ray diffraction analysis. The presence of these two elements with low oxygen indicates that the silicothermic reduction of the oxide of manganese (IV) took place. Furthermore, points 3 and 4 would be the silica obtained as a result of the silicothermic process with drags of manganese.

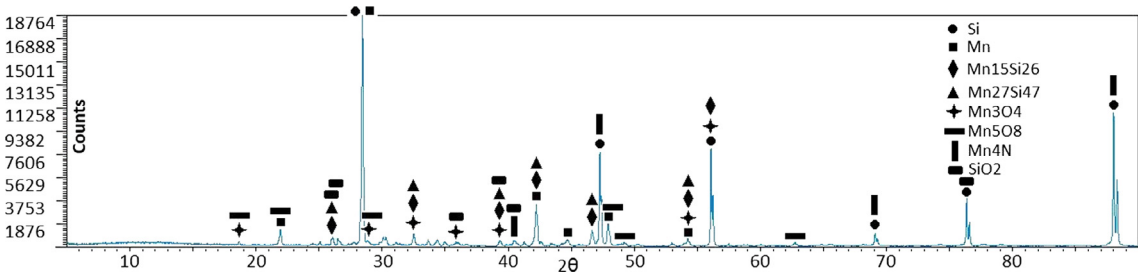

Fig. 2. X-ray diffraction pattern of the sample Mn7.

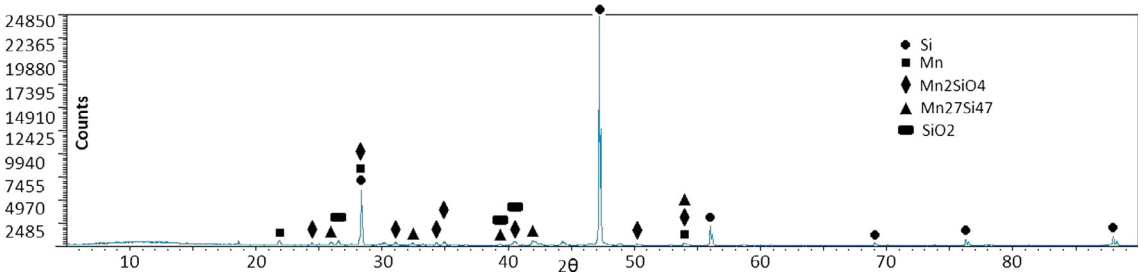

Fig. 3. X-ray diffraction pattern of the sample Mn8.

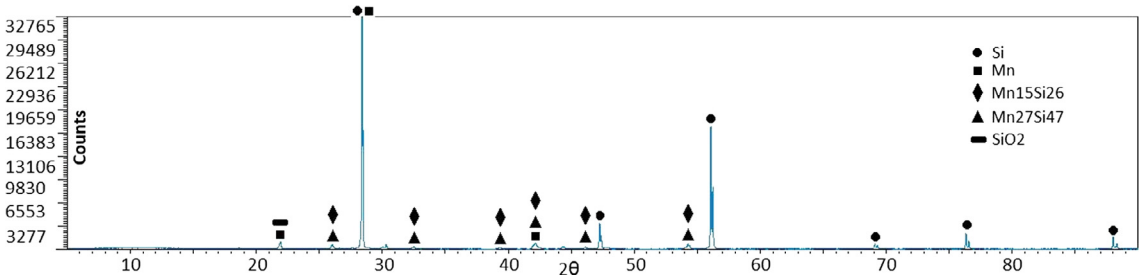

Fig. 4. X-ray diffraction pattern of the sample Bonus50.

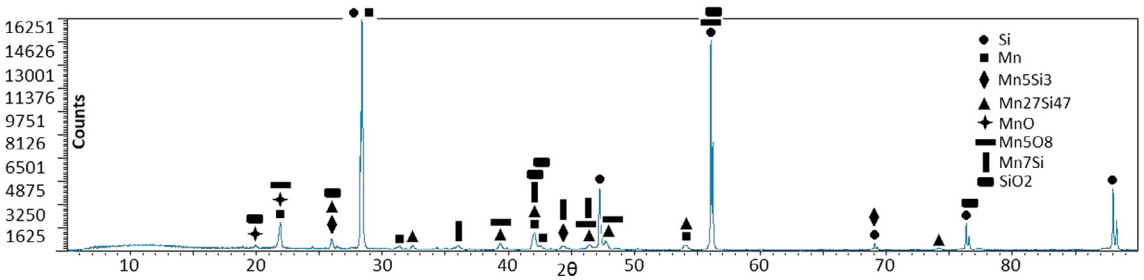

Fig. 5. X-ray diffraction pattern of the sample Mn9.

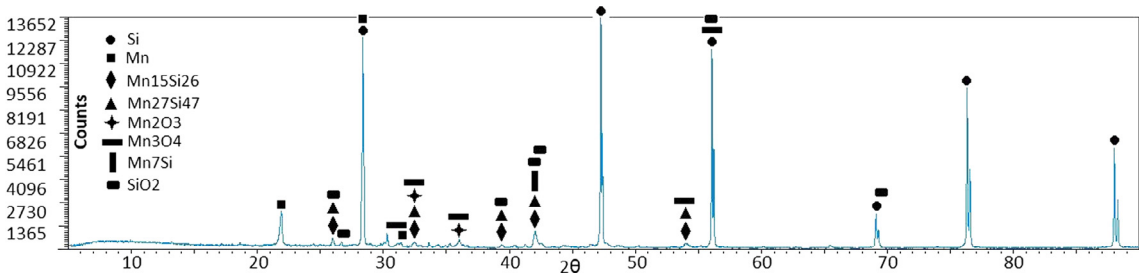

Fig. 6. X-ray diffraction pattern of the sample Mn10.

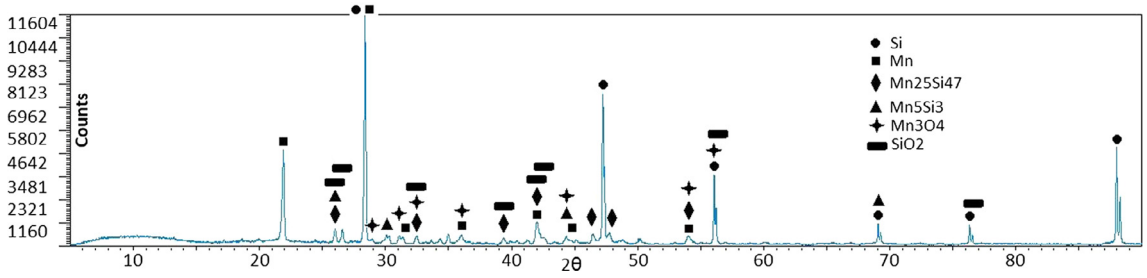

Fig. 7. X-ray diffraction pattern of the sample Bonus75.

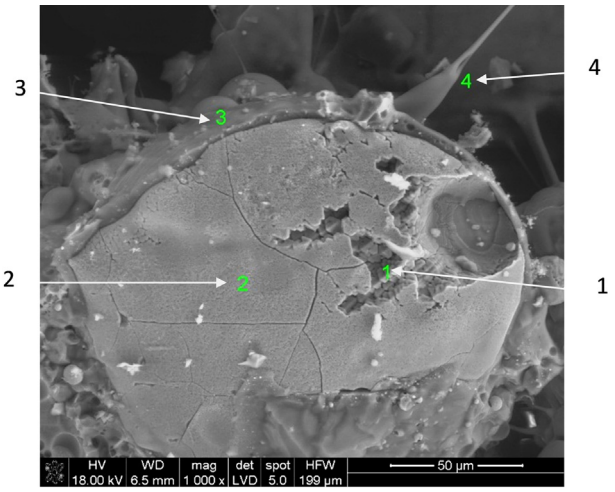

Fig. 8. SEM-EDX micrograph of the sample Mn7.

Table 1
Point analysis of the sample Mn7 (wt.%) (Fig. 8).

Element	Point 1	Point 2	Point 3	Point 4
O	3.54	4.12	40.17	40.62
Al	0.43	0.54	1.46	1.37
Si	26.63	43.49	51.23	54.13
K	0.31	0.64	0.98	1.23
Mn	69.08	51.21	6.16	2.66

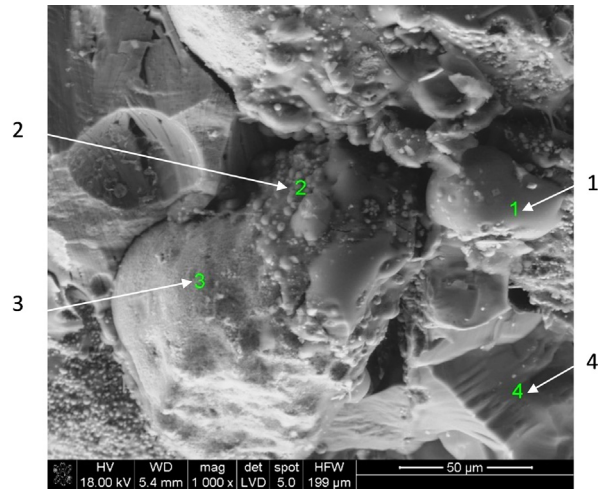

Fig. 9. SEM-EDX micrograph of the sample Mn10.

Another micrograph of the final sample (sample Mn10) is presented in the Fig. 9. The results of the point analysis are collected in the Table 2. Points 1 and 4 would show the manganese silicate. Points 2 and 3 would indicate mixtures silicon-manganese or the silicomanganese identified in the X-ray diffraction analyses. The appearance of these mixture silicon-manganese and silicomanganese is consequence of the important excesses of silicon over the stoichiometric value. Otherwise, the product of reaction would be manganese, as metallic phase, and silica, as slag. Other elements detected in the point analysis, different from the oxygen, silicon and manganese, would be impurities

Table 2
Point analysis of the sample Mn10 (wt.%) (Fig. 9).

Element	Point 1	Point 2	Point 3	Point 4
O	27.90	0.95	1.92	10.33
Al	2.67	0.85	0.35	0.98
Si	39.76	24.13	49.48	67.85
K	2.48		0.33	
Ca	0.58		0.46	
Mn	26.62	74.07	47.46	20.84

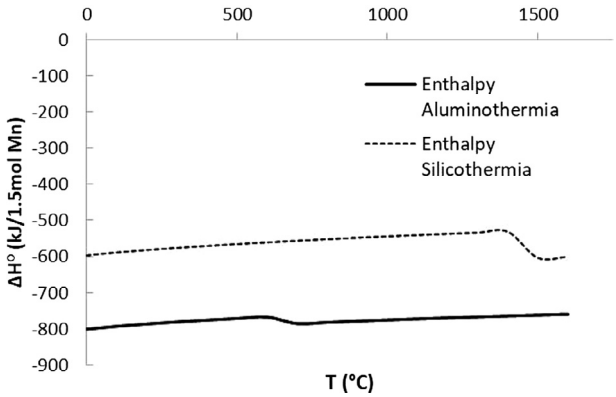

Fig. 10. Enthalpy of the manganese oxide (IV) aluminothermic and silicothermic reduction.

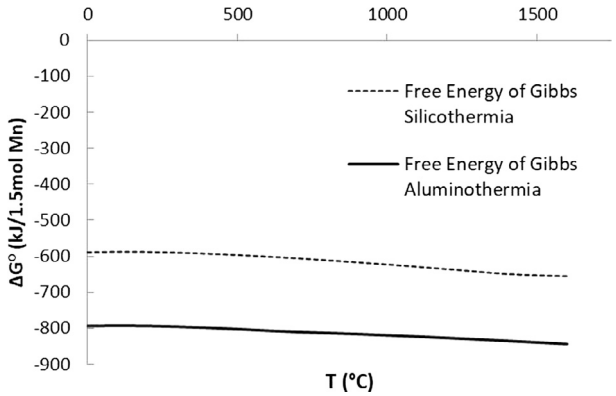

Fig. 11. Free energy of Gibbs of the manganese oxide (IV) aluminothermic and silicothermic reduction.

of the starting materials.

3.2. Discussion

The chemical reaction for the silicothermic reduction of the manganese oxide (IV) is, at room temperature, the following one:

$$MnO_2(s) + Si(s) \rightarrow Mn(s) + SiO_2(s)$$

The reaction must be initialized using a source of heat. Once initialized the process, the heat released by the own reaction should be enough to be maintained by itself (see Fig. 10, the silicothermic reduction is exothermic $\Delta H^\circ < 0$). In our case we used concentrated solar energy to initialize the reaction, but also to keep the phases in molten state. However, we have powders of the initial mixture in the crucible and, consequently, we can say that the process did no progress until the bottom of the crucible. A basic thermodynamic analysis of the reduction reaction of the manganese oxide (IV) with silicon was performed. This analysis was also done for the reduction reaction of the manganese oxide (IV) with aluminum. The analysis was done from the perspective of the enthalpy and the free energy of Gibbs, and the results are presented in the Fig. 10 (enthalpy) and Fig. 11 (free energy of Gibbs) for the reduction both with silicon and with aluminum.

Both the aluminothermic and the silicothermic reduction processes are exothermic $\Delta H^\circ < 0$, although the aluminothermic reduction is much more exothermic than the silicothermic reduction for the same quantity of manganese produced ($\Delta H^0_{Aluminothermy} < \Delta H^0_{Silicohermy}$). In the same line, the aluminothermic reduction is thermodynamically more favorable because the value of the free energy of Gibbs is more negative than in the case of the silicothermic reduction ($\Delta G^0_{Aluminothermy} < \Delta G^0_{Silicohermy}$). Thus, the aluminothermic reduction is usually employed to obtain metallic manganese. This reaction, as mentioned, is much more energetic than the silicothermic reduction of the manganese, and, it is possible to obtain manganese and slag in two separated layers adding a slag-forming element (lime) and a reagent to modify the viscosity of the system (fluorspar). However, the aluminothermic reduction of the manganese oxides, due to the energy released, is usually accompanied by a flame. The risks for the parabolic concentrator as a consequence of the limited space in the solar furnace led us to use the silicothermic reduction to produce metallic manganese instead of the aluminothermic reduction. Additionally, the method presented in this paper could be used to obtain silicomanganese, as we have checked. This alloy can replace metallic manganese and ferrosilicon in the production of some low carbon steel grades. The alloy obtained using solar energy would not have carbon due to this element is not employed in the process using the silicothermic via. The energy used to produce the alloy would come from a carbon dioxide free energy source, and, the high temperatures required for the process would be reached without paying for electricity or fossil fuels. In the same field, concentrated solar energy could be used in the obtaining of low-carbon ferromanganese. The utilization of iron (that in the industrial silicomanganese represents around 10% of the alloy) would allow reducing the liquidus temperature.

We have checked in this preliminary research that silicon-manganese mixtures and silicomanganese are obtained using concentrated solar energy and the silicothermic reduction process. Both phases are obtained even in the less favorable situation: without iron in the metallic part (that could have reduced the liquidus temperature), without slag (because slag-forming elements were not added), and without adding some reagent that could have modified the viscosity of the liquid phases.

4. Conclusions

The oxide of manganese (IV) was reduced using 99.9% silicon (50 wt% and 75 wt%) and concentrated solar energy. The silicothermic reduction was achieved under oxidizing environment, although the silicon excesses used in the experiments ensured the success of the process. However, these excesses led to the obtaining of silicon-manganese mixtures and silicomanganese at the end of the process despite the metallic manganese that was initially expected. Additionally, the short duration of the treatment together with the lack of slag-forming reagent and the viscosity of the liquid impeded the proper separation metal-slag. Solar energy could emerge as an alternative to the electrolytic via in the production of metallic manganese, or in the production of low-carbon ferroalloys, due to both the energy costs and the environmental impact. Moreover, concentrated solar energy might be used in the recovery of manganese from ferromanganese and silicomanganese slags.

Acknowledgements

Financial support by the Access to Research Infrastructures activity in the 7th Framework Program of the EU (SFERA 2 Grant Agreement no. 312643) is gratefully acknowledged and the use of the facilities and its researchers/technology experts. Project SOLMETBY (P1701250238), *Investigation and evaluation of solar energy as energy source in the treatment of metallurgical by-products*.

This research was supported by the Spanish Ministry of Education, Culture, and Sports via an FPU (Formación del Profesorado Universitario) grant to Daniel Fernández González (FPU014/02436).

References

Fernández-González, D., Ruiz-Bustinza, I., González-Gasca, C., Piñuela-Noval, J., Mochón-Castaños, J., Sancho-Gorostiaga, J., Verdeja, L.F., 2018a. Concentrated solar energy applications in materials science and metallurgy. Sol. Energy 180, 520–540.

Fernández-González, D., Prazuch, J., Ruiz-Bustinza, I., González-Gasca, C., Piñuela-Noval, J., Verdeja, L.F., 2018b. Solar synthesis of calcium aluminates. Sol. Energy 171, 658–666.

Fernández-González, D., Prazuch, J., Ruiz-Bustinza, I., González-Gasca, C., Piñuela-Noval, J., Verdeja, L.F., 2018c. Iron metallurgy via concentrated solar energy. Metals-Basel 8, 873.

Fernández-González, D., Sancho-Gorostiaga, J., Piñuela-Noval, J., Verdeja González, L.F., 2018d. Anodic lodes and scrapings as a source of electrolytic manganese. Metals-Basel 8, 162.

Fernández-González, D., Prazuch, J., Ruiz-Bustinza, I., González-Gasca, C., Piñuela-Noval, J., Verdeja, L.F., 2019a. The treatment of Basic Oxygen Furnace (BOF) slag with concentrated solar energy. Sol. Energy 180, 372–382.

Fernández-González, D., Prazuch, J., Ruiz-Bustinza, I., González-Gasca, C., Piñuela-Noval, J., Verdeja, L.F., 2019b. Transformations in the Si-O-Ca system: Silicon-calcium via solar energy. Sol. Energy 181, 414–423.

Haque, N., Norgate, T., 2013. Estimation of greenhouse gas emissions from ferroalloy production using life cycle assessment with particular reference to Australia. J. Clean. Prod. 39, 220–230.

Holappa, L., 2013. Basics of ferroalloys. In: Gasic, M. (Ed.), Handbook of Ferroalloys. Theory and Practice. Butterworth-Heinemann, Oxford, pp. 9–28.

Heo, J.H., Park, J.H., 2018. Manganese recovery by silicothermic reduction of MnO in BaO-MnO-MgO-CaF_2 (-SiO_2) slags. Metall. Mater. Trans. B 49, 514–518.

Jamieson, B.J., Coley, K.S., 2017. Kinetics of Silicothermic reduction of manganese oxide for advanced high-strength steel production. Metall. Mater. Trans. B 48, 1613–1624.

Mochón, J., Ruiz-Bustinza, I., Vázquez, A., Fernández, D., Ayala, J.M., Barbés, M.F., Verdeja, L.F., 2014. Transformations in the iron-manganese-oxygen-carbon system resulted from treatment of solar energy with high concentration. Steel Res. Int. 85, 1469–1476.

Ndlovu, S., Simate, G.S., Matinde, E., 2017. Waste Production and Utilization in the Metal Extraction Industry, first ed. CRC Press (Taylor & Francis Group), Boca Raton.

Olsen, S.E., Tangstad, M., Lindstad, T., 2007. Production of Manganese Ferroalloys, first ed. Tapir Akademisk Forlag, Trondheim.

Ruiz-Bustinza, I., Cañadas, I., Rodríguez, J., Mochón, J., Verdeja, L.F., García-Carcedo, F., Vázquez, A., 2013. Magnetite production from steel wastes with concentrated solar energy. Steel Res. Int. 84, 207–217.

Sakamoto, Y., Tonooka, Y., Yanagisawa, Y., 1999. Estimation of energy consumption for each process in the Japanese steel industry: a process analysis. Energy Convers. Manage. 40, 1129–1140.

Tangstad, M., 2013. Major (bulk) ferroalloys. In: Gasic, M. (Ed.), Handbook of Ferroalloys. Theory and Practice. Butterworth-Heinemann, Oxford, pp. 179–221.

Zhang, W., Cheng, Z., 2007. Manganese metallurgy review. Part I: Leaching of ores/secondary materials and recovery of electrolytic/chemical manganese dioxide. Hydrometallurgy 89, 137–159.